

See discussions, stats, and author profiles for this publication at: <https://www.researchgate.net/publication/285745789>

High fat diet-induced diabetes in mice exacerbates cognitive deficit due to chronic hypoperfusion

Article in *Journal of Cerebral Blood Flow & Metabolism* · November 2015

DOI: 10.1177/0271678X15616400

CITATIONS

3

READS

128

12 authors, including:



[Wenri Zhang](#)

Oregon Health and Science University

53 PUBLICATIONS 1,081 CITATIONS

[SEE PROFILE](#)



[Martin Pike](#)

Oregon Health and Science University

48 PUBLICATIONS 1,615 CITATIONS

[SEE PROFILE](#)



[Jacob Raber](#)

Oregon Health and Science University

224 PUBLICATIONS 7,821 CITATIONS

[SEE PROFILE](#)



[Nabil J Alkayed](#)

Oregon Health and Science University

155 PUBLICATIONS 4,960 CITATIONS

[SEE PROFILE](#)

Some of the authors of this publication are also working on these related projects:



Low dose radiation [View project](#)



diabetic foot ulcer [View project](#)

All content following this page was uploaded by [Nabil J Alkayed](#) on 07 December 2015.

The user has requested enhancement of the downloaded file. All in-text references [underlined in blue](#) are added to the original document and are linked to publications on ResearchGate, letting you access and read them immediately.

High fat diet-induced diabetes in mice exacerbates cognitive deficit due to chronic hypoperfusion

Kristen L Zuloaga¹, Lance A Johnson^{2,3}, Natalie E Roese¹, Tessa Marzulla³, Wenri Zhang¹, Xiao Nie¹, Farah N Alkayed¹, Christine Hong¹, Marjorie R Grafe^{1,4}, Martin M Pike⁵, Jacob Raber^{2,3} and Nabil J Alkayed^{1,2}

Abstract

Diabetes causes endothelial dysfunction and increases the risk of vascular cognitive impairment. However, it is unknown whether diabetes causes cognitive impairment due to reductions in cerebral blood flow or through independent effects on neuronal function and cognition. We addressed this using right unilateral common carotid artery occlusion to model vascular cognitive impairment and long-term high-fat diet to model type 2 diabetes in mice. Cognition was assessed using novel object recognition task, Morris water maze, and contextual and cued fear conditioning. Cerebral blood flow was assessed using arterial spin labeling magnetic resonance imaging. Vascular cognitive impairment mice showed cognitive deficit in the novel object recognition task, decreased cerebral blood flow in the right hemisphere, and increased glial activation in white matter and hippocampus. Mice fed a high-fat diet displayed deficits in the novel object recognition task, Morris water maze and fear conditioning tasks and neuronal loss, but no impairments in cerebral blood flow. Compared to vascular cognitive impairment mice fed a low fat diet, vascular cognitive impairment mice fed a high-fat diet exhibited reduced cued fear memory, increased deficit in the Morris water maze, neuronal loss, glial activation, and global decrease in cerebral blood flow. We conclude that high-fat diet and chronic hypoperfusion impair cognitive function by different mechanisms, although they share common features, and that high-fat diet exacerbates vascular cognitive impairment pathology.

Keywords

Vascular cognitive impairment, vascular dementia, diabetes, high-fat diet, cerebral blood flow, cognitive impairment, chronic cerebral hypoperfusion

Received 31 July 2015; Revised 22 September 2015; Accepted 30 September 2015

Introduction

Vascular cognitive impairment (VCI) is the second most common cause of dementia. Endothelial injury is thought to be responsible for initiating microvascular hypoperfusion and subsequent VCI. Endothelial dysfunction can be caused by a variety of vascular risk factors such as hypertension, smoking, and diabetes. In humans, diabetes increases VCI risk two-fold, an effect that has largely been attributed to diabetes-induced vascular dysfunction.^{1,2} There is also evidence of increased cognitive dysfunction in multiple cognitive domains of type 2 diabetic individuals.³ Several potential factors that may contribute to these cognitive

¹Department of Anesthesiology and Perioperative Medicine, Oregon Health and Science University, Portland, OR, USA

²The Knight Cardiovascular Institute, Portland, OR, USA

³Department of Behavioral Neuroscience, Portland, OR, USA

⁴Department of Pathology, Portland, OR, USA

⁵Advanced Imaging Resource Center, Oregon Health and Science University, Portland, OR, USA

Corresponding author:

Nabil J Alkayed, Department of Anesthesiology and Perioperative Medicine, The Knight Cardiovascular Institute, Oregon Health and Science University, 3181 SW Sam Jackson Park Road, UHN-2 Portland, OR 97239, USA.

Email: alkayedn@ohsu.edu

deficits include reduced endothelial function, greater incident of white matter damage, lower cerebral blood flow (CBF), increased brain atrophy, increased infarcts and reduced neuroprocessing.^{1,2,4} The relative contribution of each of these pathologies and whether these pathologies are due to hyperglycemia or due to common comorbidities such as vascular disease is unknown.

Cognitive impairment and vascular dysfunction have also been reported in rodent models of diabetes. A common mouse model of type 2 diabetes is long-term high-fat (HF) diet which causes insulin resistance and impaired glucose tolerance.⁵ Mice administered an HF diet exhibit cognitive deficits in learning and memory tasks^{6,7} and decreased cerebrovascular endothelial function.⁸

Despite evidence that diabetes causes endothelial dysfunction, it is unknown whether this endothelial dysfunction causes reductions in CBF that lead to cognitive impairment or if diabetes causes cognitive impairment regardless of changes in CBF. In order to address this issue, we used a chronic HF diet to model type 2 diabetes⁵ and unilateral common carotid artery occlusion (UCCAO) to induce chronic cerebral hypoperfusion and model VCI.^{9–13} We sought to determine if the effects of VCI and diabetes on cognitive function were similar and whether HF diet/diabetes would exacerbate specific cognitive impairments induced by chronic cerebral hypoperfusion in mice.

Materials and methods

This study was conducted in accordance with the National Institutes of Health guidelines for the care and use of animals in research, and protocols were approved by the Institutional Animal Care and Use Committee at Oregon Health and Science University, Portland, OR, USA. Reporting of the results conforms to the ARRIVE (Animal Research Reporting in Vivo Experiments) guidelines.

Animals and experimental design

Male C57BL/6J mice were purchased from Jackson laboratories (Bar Harbor, Maine). An overview of the experimental timeline is presented in Figure 1. At 6 weeks of age, mice were placed on either a HF diet (60% fat; D12492, Research Diets, New Brunswick, NJ) or a low fat control diet (10% fat, D12450B, Research Diets) ($n = 30$ per group). All mice received numerical tail tattoos (1–60) to serve as identifiers. Mice remained on their respective diets until the end of the study. After 3 months on the diet, mice were subjected to a glucose tolerance test (GTT), allowed to recover for 2 weeks, then received UCCAO

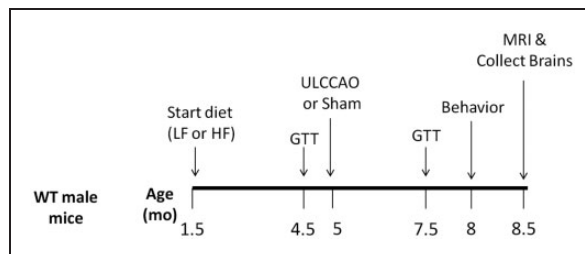


Figure 1. Experimental timeline. Male mice were placed on a high fat (HF) diet or control low fat (LF) diet ($n = 30$ per group). Three months later, mice were subjected to glucose tolerance tests (GTT), allowed to recover, then subjected to right UCCAO (VCI) or sham surgery ($n = 15$ per group). Three months later GTTs were repeated. Next, behavioral performance was assessed using the open field test, novel object recognition test, Morris water maze, and cued and contextual fear conditioning tests ($n = 13–15$ per group). Finally, mice received magnetic resonance imaging ($n = 7$ per group, randomly selected), were perfused and brains collected for histological analysis ($n = 7$ per group).

($n = 15$ mice per group) or sham surgery ($n = 15$ mice per group). The survival rate 1 month following surgery was 100%. Two out of 30 mice on the HF diet were killed in the final month of the study due to severe skin dermatitis. After 6 months on the diet, mice received a second GTT, were allowed to recover for 2 weeks, and then underwent behavior testing. Upon completion of behavior testing, mice were either euthanized or underwent magnetic resonance imaging (MRI) ($n = 7$ per group, randomly selected). Following MRI, mice were perfused with paraformaldehyde and brains collected for histological analysis. Mice were group-housed until behavior testing was performed, at which point they were singly housed until the end of the study. Behavior testing and MRI were completed by experimenters blinded to whether mice were in the sham or VCI treatment group. Due to differences in food color and mouse appearance, diabetic status could not be blinded during behavior testing or MRI. All data analysis was done by experimenters blinded to both diabetic status and surgery. Sample sizes needed were calculated based on previous experience with methods used.

GTT

At 3 and 6 months post-dietary intervention, mice were fasted overnight and baseline blood glucose levels in saphenous vein blood were measured by glucometer (Breeze 2, Bayer, Tarrytown, NY). Each mouse received 2 g/kg of glucose via oral gavage and blood glucose levels were re-measured at 10, 20, 30, 60, 90, and 120 min.

UCCAO

Right UCCAO or sham surgery was performed 3 months after dietary intervention using aseptic techniques. Mice were randomly assigned to surgical group. Mice were anesthetized with 2% isoflurane and kept warm with water pads. After midline cervical incision, the right common carotid artery was isolated and two 6–0 silk sutures were placed under the carotid. For VCI mice, the two ties were tightly tied and the carotid was cauterized between the two ties and cut. For sham mice, the ties were removed from under the carotid arteries without being tied and vessels were not cauterized. For all mice, incisions were closed and mice were allowed to recover. Mice returned to their group housed caging after recovering from anesthesia. The survival rate was 100%.

Behavioral and cognitive testing

Three months after VCI or sham surgery mice were tested for exploratory activity and anxiety in the open field (day 1), habituated to the open field on days 2 and 3, tested for novel object recognition task (NORT) on days 4 and 5, spatial learning and memory in the Morris water maze (MWM) on days 8–12, and contextual and cued fear conditioning on days 15 and 16. Behavior testing was performed as described previously¹³ and detailed below.

Open field. Mice were placed into a square arena (40.64 × 40.64 cm) and allowed to explore for 10 min. Behavioral performance was tracked and scored using an automated video system (Ethovision 7.0 XT, Noldus, Sterling, VA). Exploratory behavior was analyzed using total distance moved (cm) as outcome measure. Time spent in the more anxiety-provoking center of the open field was analyzed as well.

Novel object recognition. Mice were habituated to the open field described above over 3 days, one 10-min trial per day. On day 4, the mice were exposed to the arena containing two identical objects. On day 5, one of the two identical objects (henceforth “familiar”) was replaced by a novel object. Performance of the mice was video recorded. Orientation to the object, within 2 cm proximity, as well as interaction with the object (climbing, sniffing, and pushing) was defined as exploring the object. Novel object recognition and discrimination was calculated as the percent time spent exploring the novel object out of the total time spent exploring both objects. Distance moved was analyzed using automated multiple body point video tracking (Ethovision XT 7.0, Noldus Information Technology, Wageningen,

the Netherlands), using parameters previously described and validated.¹⁴

Water maze. Hippocampus-dependent spatial learning and memory was assessed using a version of the MWM. The maze consisted of a circular pool (diameter 140 cm), filled with opaque water (24°C), divided conceptually into four quadrants. Mice were first trained to locate an “escape” platform (plexiglass circle, 6 cm radius) submerged 2 cm below the surface of the water and made visible by the use of a cue (a colored cylinder, 2.5 cm radius, 8 cm height) during the “visible” trials (days 1 and 2). For the visible platform training days, there were two daily sessions, morning and afternoon, which were separated by an intersession interval of 3 h. Each session consisted of two trials, with 5-min intertrial intervals. Mice were placed into the water facing the edge of the pool in one of nine randomized locations (consistent for each mouse). A trial ended when the mouse located the platform. Mice that failed to locate the platform within 60 s were led to the platform by placing a finger in front of their swim path. Mice were taken out of the pool after they remained on the platform for a minimum of 10 s. During the visible platform sessions, the location of the platform was moved between each of the four quadrants to avoid procedural biases in task learning. Subsequent to the visual trials, mice were trained to locate a hidden platform, requiring the mice to rely on extra maze cues for spatial reference and orientation. Extra-maze cues consisted of four large (50 × 50 cm) cues of different shapes and color combinations, positioned at the borders of the four quadrants. Cues were placed 100 cm from the ground, and 90 cm away from the edge of the pool. The platform was not rotated during the hidden platform trials and remained in the same location. Twenty four hours after the last trial of hidden platform training, spatial memory retention of the mice was assessed in a “probe” trial (no platform). During the probe trials, mice were placed into the water in the quadrant opposite of the target quadrant. The time spent in the target quadrant compared to the time spent in the three nontarget quadrants was analyzed. The swimming patterns of the mice were recorded with Noldus Ethovision video tracking software (Ethovision XT, Noldus Information Technology, Wageningen, the Netherlands) set at six samples/s. The time to locate the platform (latency) was used as a measure of performance for the visible and hidden platform sessions. Latency to reach the target was measured in seconds, and was calculated for each session by averaging values from the two within-session trials. Because swim speeds can influence the time it takes to reach the platform, they were also analyzed.

Fear conditioning. In this task, mice learn to associate a conditioned stimulus (CS, e.g. the environmental context, or a discrete cue) with a mild foot shock (unconditioned stimulus, US). CS–US pairings are preceded by a short habituation period, during which a baseline measure of locomotor activity is analyzed. Freezing, defined as immobility with the exception of respiration, is considered a post-exposure fear response, and is a widely used indicator of conditioned fear.¹⁵ Mice were trained and tested using a Med Associates mouse fear conditioning system containing VideoFreeze automated scoring system (Med Associates, St. Albans, Vermont), as described previously in detail and validated against traditional hand scoring methods (Anagnostaras et al., 2010). On day 1, the mice were placed inside a dark fear-conditioning chamber. Chamber lights (at 100 lux) turned on at 0 s, followed by a 90-s habituation period and a subsequent 30-s (2800 Hz, 80 dB) tone (cue). A 2-s 0.7 mA foot shock was administered at 28 s, co-terminating with the tone at 30 s. After a 30-s inter-stimulus interval the tone-shock pairing were repeated for a total of five tone-shock pairings. On day 2, hippocampus dependent associative learning was assessed during reexposure to the training environment for 300 s. Three hours later, mice were exposed to a modified environment (scented with vanilla extract, cleaned with 10% isopropanol instead of 0.5% glacial acetic acid, novel floor texture covering the shock-grid, and rounded walls). They were allowed to habituate for 90 s, and then exposed to the cue for a second period of 180 s. Associative learning was measured as the percent time spent freezing in response to the contextual environment or the tone. Immediate acquisition of conditioned fear was measured following CS–US pairings. Motion during shock (proprietary index, Med Associates) was measured to assess potential differences in response to the shock during training.

MRI

Imaging was conducted following behavioral and cognitive testing, 3.5 months after VCI or sham surgery. Power analysis revealed that only seven mice were needed per group for MRI/histology measures, in contrast to the 12 mice per group needed for behavioral studies. The difference is mostly attributed to inherent variability in behavioral endpoints, compared to CBF and histology. Because of the difference in variability and cost associated with MRI, we have limited the number of mice that went on to this portion of the study to seven mice per group. Mice were randomly assigned to receive MRI based on tail tattoo number. Tail tattoo numbers were assigned prior to any dietary or surgical intervention. All mice that received MRI

also were processed for histology. For MRI studies, mice were anesthetized with a ketamine/xylazine mixture (1.5 mg xylazine/10 mg ketamine/100 g). MR imaging employed a Bruker-Biospin 11.75 T small animal MR system with a Paravision 5.1 software platform, 9-cm inner diameter gradient set (750 mT/m), with a 72 mm (ID) RF resonator and an actively decoupled 20 mm Bruker surface coil for transmit/receive. The mice were positioned with their heads immobilized on a custom platform/head holder. Body temperature of the mice was monitored and maintained at 37°C using a warm air temperature control system (SA instruments). Isoflurane (0.5–2%) in 100% oxygen was administered and adjusted while monitoring respiration. A coronal 25-slice T₂-weighted image set was obtained (Paravision spin echo RARE, 256 × 256 matrix, 125 μm in-plane resolution, 0.5 mm slice width, TR 4000 ms, TE_{effective} 46.8 ms, RARE factor 8, 2 averages). A coronal 20 slice T₂-weighted image set was then obtained, employing 8 echoes with 15 ms spacing, (Paravision spin echo RARE, 256 × 256 matrix, 125 μm in-plane resolution, 0.5 mm slice width, TR 3500 ms). T₂ maps were generated by performing a pixel by pixel fit of the decaying image intensity to the function $(SI(t) = SI_0 e^{-t/T_2})$. CBF was measured using arterial spin labeling (ASL), employing the flow-sensitive alternating inversion recovery rapid acquisition with relaxation enhancement pulse sequence (Paravision FAIR-RARE), with TE/TR = 45.2/10000 ms, FOV = 3.5 cm, slice thickness = 2 mm, number of slices = 1, matrix = 128 × 128, RARE factor = 72, and 23 turbo inversion recovery values ranging from 40 to 4400 ms. This sequence labels the inflowing blood by global inversion of the equilibrium magnetization.¹⁶ The T₂ images were employed to accurately place the coronal ASL flow slice at the same position in each mouse, posterior to the lateral ventricles, and 2 mm anterior to the anterior commissure.

Image processing

The Jim image analysis software (Xinapse Systems) was employed for image processing. CBF maps (in units of ml/100-min) were generated using the Bruker ASL perfusion processing macro which employs the equation: where λ is the blood brain partition coefficient (=0.9), T_{1blood} is the T₁ of blood (=2800 ms) and T_{1sel} and T_{1nonsel} are the measured T₁ values under selective and nonselective inversion conditions, respectively. CBF maps were exported into Jim imaging software for further processing. The multiplanar reconstruction tool in Jim was used to accurately align the T₂ maps and T₂ image sets to the coronal plane of view. A T₂ threshold of 40 ms guided the manual drawing of

regions of interest (ROIs) around ventricles on the T_2 maps. Ventricular volume quantification included the lateral ventricles, and the third and fourth ventricles, to a point 1.5 mm posterior to the anterior commissure. Hippocampal volume between the anterior commissure and a point 1.5 mm anterior to it was calculated using ROIs created on three contiguous T_2 image slices. Various ROIs were created on the ASL CBF maps to assess CBF in those regions. Mean hemispheric CBF values were determined with ROIs encompassing the entire hemisphere, with an erosion of 1 pixel from the brain circumference to exclude brain surface vasculature. Using the Allen Institute Mouse Brain atlas¹⁷ as a guide, regional ROIs of the cortex, striatum, corpus callosum, and a medial portion of the hippocampus, were created in T_2 maps at a position 2 mm anterior of the anterior commissure and transferred to the corresponding location in CBF maps. Hippocampal ROIs were drawn to minimize partial volume effects from ventricular regions contained within the 2-mm ASL imaging slice.

Histology

Mice were euthanized after having undergone behavior testing and MRI. The animals were perfused with 0.9% saline followed by 4% paraformaldehyde. After removal from the skull, the brains were fixed for 24 h in 4% paraformaldehyde then dehydrated and cleared (using Prosoft and Propar, Anatech Ltd, Battle Creek, MI) for paraffin embedding. Serial six micron thick sections were cut through the entire extent of the hippocampus and amygdala. For immunohistochemistry, deparaffinized sections were heated in 10 mM citrate buffer at pH 6.0 in a steamer for 30 min for antigen retrieval. All rinses were with Tris-buffered saline (TBS), pH 7.6. Sections were incubated with 4% normal donkey serum in phosphate-buffered saline with 1% bovine serum albumin and 0.3% Triton (blocking serum) for 60 min at room temperature to block nonspecific binding of the secondary antibodies. For the GFAP stains, sections were blocked using the Vector Mouse-on-Mouse kit (BMK-2202, Vector Laboratories, Burlingame, CA). Sections were incubated with the primary antibodies (mouse anti-GFAP 1:500, #MAB360 EMD Millipore, Billerica, MA; rabbit polyclonal anti-Iba-1 1:1000, #019-19741 Wako Chemicals, Richmond, VA; rabbit anti-NeuN 1:500, #ABN78 EMD Millipore) diluted in the blocking serum, overnight at 4°C. The fluorescent-labeled secondary antibodies (Alexa Fluor 594 conjugated donkey anti-mouse 1:250, #A21203 Life Technologies, Eugene, OR; Alexa Fluor conjugated donkey anti-rabbit 1:500, #A21206 Life Technologies; rhodamine conjugated donkey anti-rabbit 1:300, #711-295-152 Jackson ImmunoResearch, West Grove, PA)

diluted in the blocking serum), were applied to the tissue for 150 min at room temperature. The sections were counterstained with Hoechst 33342 (Molecular Probes, 1:3000, Eugene, OR), coverslipped with Fluoromount-G (Southern Biotech, Birmingham, AL), and imaged with a fluorescence microscope. All analysis was conducted by experimenters blinded to the both surgical group and to dietary intervention group using Image J software. For quantification of NeuN, a ROI of uniform size was placed over a high magnification (400×) image of the dentate gyrus and cells were counted manually. For quantification density of Iba-1 and GFAP staining, a threshold was set in Image J so that only immunoreactive cells were highlighted and area covered within an ROI of a standard size was calculated for each brain region.

Statistical analysis

Data are expressed as mean \pm SEM. All data were tested for sphericity (Mauchly's test) and Greenhouse–Geisser corrections were made for tests of within-subjects effects when necessary. Groups were compared by two-way ANOVA with Holm-Sidak's *post hoc* test using Prism (GraphPad Software, La Jolla, CA). Differences were considered significant at $p < 0.05$. We expected a priori hemisphere differences as only the right carotid was occluded causing a unilateral injury; therefore data for the two hemispheres were analyzed separately. Novel object preference was first analyzed using two-way ANOVA comparing the novel and familiar object and genotype, followed by *t*-tests to compare against a hypothetical value (no preference, 50%). Water maze learning curves and fear conditioning were analyzed using repeated measures two-way ANOVA.

Results

Mice on a long-term HF diet develop a diabetic phenotype

A long-term HF (60% fat) diet was used to model type 2 diabetes in mice.⁵ Prior to dietary intervention, there were no differences in body weight (Figure 2(a)) or fasting blood glucose levels between groups. Mice were placed on HF or low fat (LF; 10% fat) diet of equal caloric content. HF diet caused a significant increase in body weight after only 6 weeks on the diet (Figure 2(b)). After 3 months on the diet, a GTT was performed. Mice on the HF diet showed a greater increase in blood glucose levels following oral gavage of glucose and a slower rate of clearance of the glucose from their blood (Figure 2(c)). After 6 months on the diet, HF mice displayed elevated fasting blood glucose

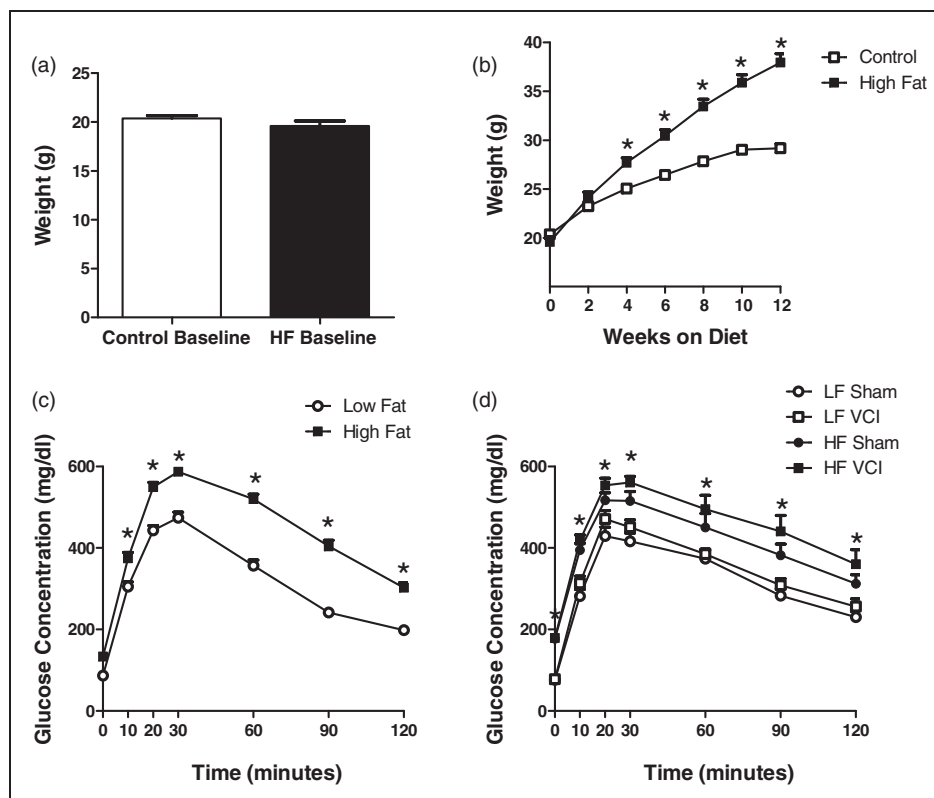


Figure 2. Mice on a long-term high fat diet develop a diabetic phenotype. Young (1.5-month-old) male mice were placed on a high fat (HF) diet or control low fat (LF) diet. (a) Prior to initiation of dietary intervention there were no differences in body weight between groups. (b) HF diet caused an increase in body weight after 6 weeks on the diet which persisted as weight gain plateaued after 12 weeks (* $p < 0.001$ vs. LF). $N = 30$ per group. (c) After 3 months on the HF diet, fasting blood glucose levels were slightly elevated (time 0), however; clearance of glucose was greatly impaired ($p < 0.001$ vs. LF), $N = 30$ per group. (d) After 6 months on the HF diet, fasting blood glucose levels were significantly elevated and glucose clearance was significantly impaired in HF compared to LF diet mice, regardless of VCI or sham surgery ($p < 0.01$ vs. LF sham). $N = 13$ – 15 per group.

levels, increased blood glucose levels following glucose challenge, and impaired glucose clearance (Figure 2(d)) compared to LF mice, regardless of UCCAO or sham surgery.

UCCAO and HF diet cause cognitive impairments; HF diet exacerbates specific impairments following UCCAO

Three months after right UCCAO or sham surgery, mice underwent behavioral and cognitive testing. Neither HF diet nor VCI surgery caused alternations in activity or the amount of time spent in the center of the field (data not shown). Non-spatial memory was assessed using the NORT. Sham mice showed a clear preference for the novel object but VCI mice did not show a preference, suggesting impairment in recognition memory (Figure 3(a)). Mice on an HF diet, both in the sham and UCCAO groups, also failed to show a preference for the novel object, suggesting a non-spatial memory deficit (Figure 3(a)). Next, spatial learning and memory was assessed in the MWM. During the training

phase, both when the platform was visible and when it was hidden, mice on an HF diet, regardless of UCCAO or sham surgery, performed more poorly, indicating impairments in task learning as well (Figure 3(b)). Both HF VCI and HF sham mice performed poorer during the probe trial, with fewer crossings over the target, suggesting deficits in spatial memory retention (Figure 3(c)). Finally, mice were subjected to both cued and contextual fear conditioning tasks. No differences were detected between groups in the contextual fear conditioning task. However, both HF Sham mice and HF VCI mice showed impairments in cued fear memory compared to LF Sham mice (Figure 3(d)).

LF VCI mice show a unilateral decrease in CBF, while HF VCI mice also display a global decrease in CBF that is exacerbated in the ischemic hemisphere

We determined the effect of HF, UCCAO, or a combination of both insults on CBF. After 6.5 months on their respective diets, there were no differences in CBF between HF and LF diet mice that received a sham

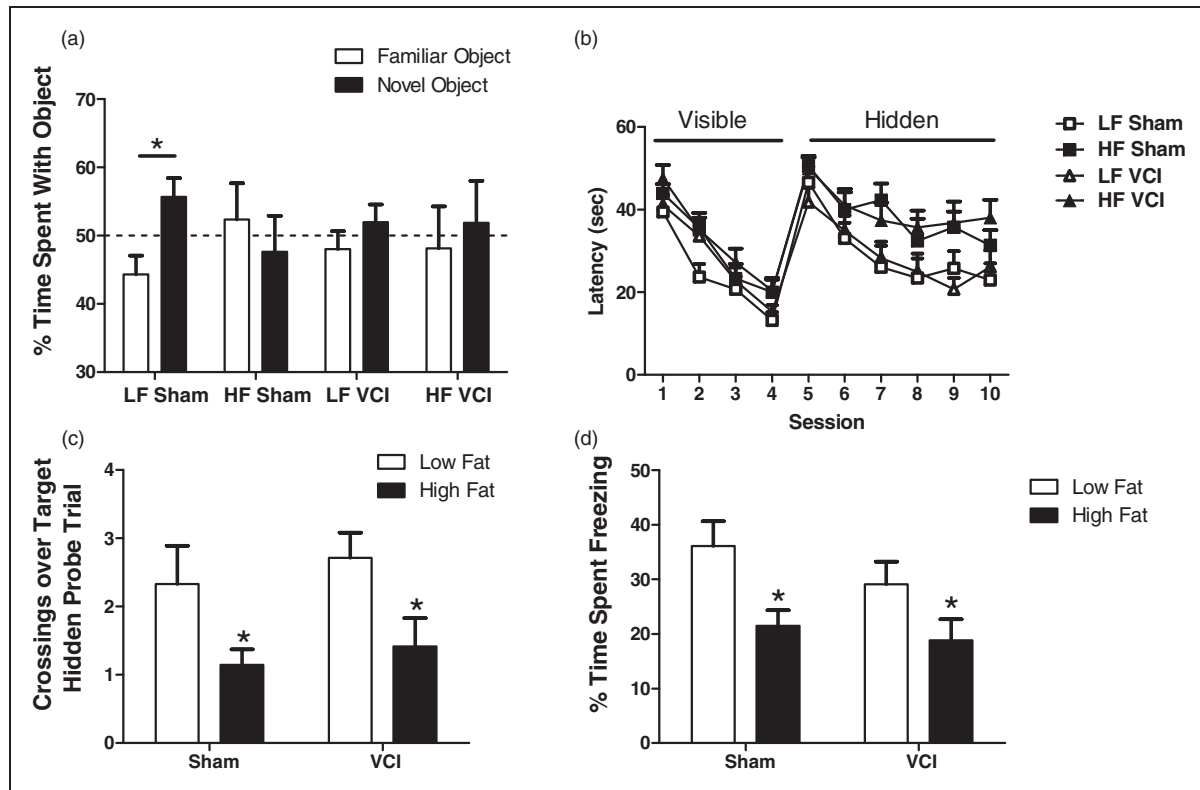


Figure 3. UCCAO and HF diet cause cognitive impairments; HF diet exacerbates specific impairments following UCCAO. (a) LF Sham mice showed a clear preference for the novel object in the NORT, while HF Sham, LF VCI, and HF VCI mice did not (* $p < 0.01$ vs. familiar object). (b) During both the visible and hidden platform phases of MWM task learning HF diet mice, regardless of sham or VCI surgery, performed more poorly ($p < 0.01$ vs. LF). (c) During the probe trial of the MWM, both HF Sham and HF VCI mice showed a reduced number of crossings over the hidden platform target location (* $p < 0.05$ vs. LF Sham). (d) During the cued fear conditioning memory task, both HF Sham and HF VCI mice showed less freezing during the tone stimulus (* $p < 0.05$ vs. LF Sham). $N = 13$ – 15 per group for all cognitive tasks.

surgery (Figure 4(a) to (c)). LF VCI mice showed a decrease in CBF in the right (ischemic) hemisphere compared to the left hemisphere that was not present in sham mice (Figure 4(a) and (b)), but showed no differences in total CBF (Figure 4(c)). VCI mice fed an HF diet showed both a decrease in CBF in the right hemisphere compared the left and also a global decrease in CBF that was not present in LF VCI mice (Figure 4(a) to (c)). There were no differences in CBF in the left (non-ischemic) hemisphere (data not shown). When CBF was analyzed specifically in the hippocampus, a region involved in spatial learning and memory, HF diet again showed no effect on CBF, with VCI surgery causing a deficit (Figure 4(d) and (e)). There were no differences in hippocampal CBF in the left (non-ischemic) hemisphere (data not shown).

VCI mice have an increase in white matter reactive changes, which is exacerbated by HF diet

White matter damage is commonly observed in VCI patients.¹⁸ In rodents, one of the most prominent

white matter tracks is the corpus callosum (CC). HF diet alone did not alter Iba-1 or GFAP immunoreactivity in the CC (Figure 5(a) to (c)). However, VCI surgery increased expression of both of these markers in the ischemic hemisphere (Figure 5(a) and (c)). HF VCI mice showed the greatest increase in both Iba-1 and GFAP in the ischemic hemisphere (Figure 5(b), (d) and (e)). Despite increases in Iba-1 and GFAP expression in the CC, we did not detect any gross abnormalities in myelination, as measured by eriochrome staining (data not shown).

VCI mice display reactive changes and neuronal loss, some of which are exacerbated by HF diet

The hippocampus is a key brain region for spatial learning and memory. Loss of neurons or atrophy of this area is associated with dementia.¹⁹ We found that neither HF diet nor VCI surgery caused changes in hippocampal size on MRI T2 images (data not shown). We also examined expression of Iba-1 and GFAP in the CA1 region of the hippocampus.

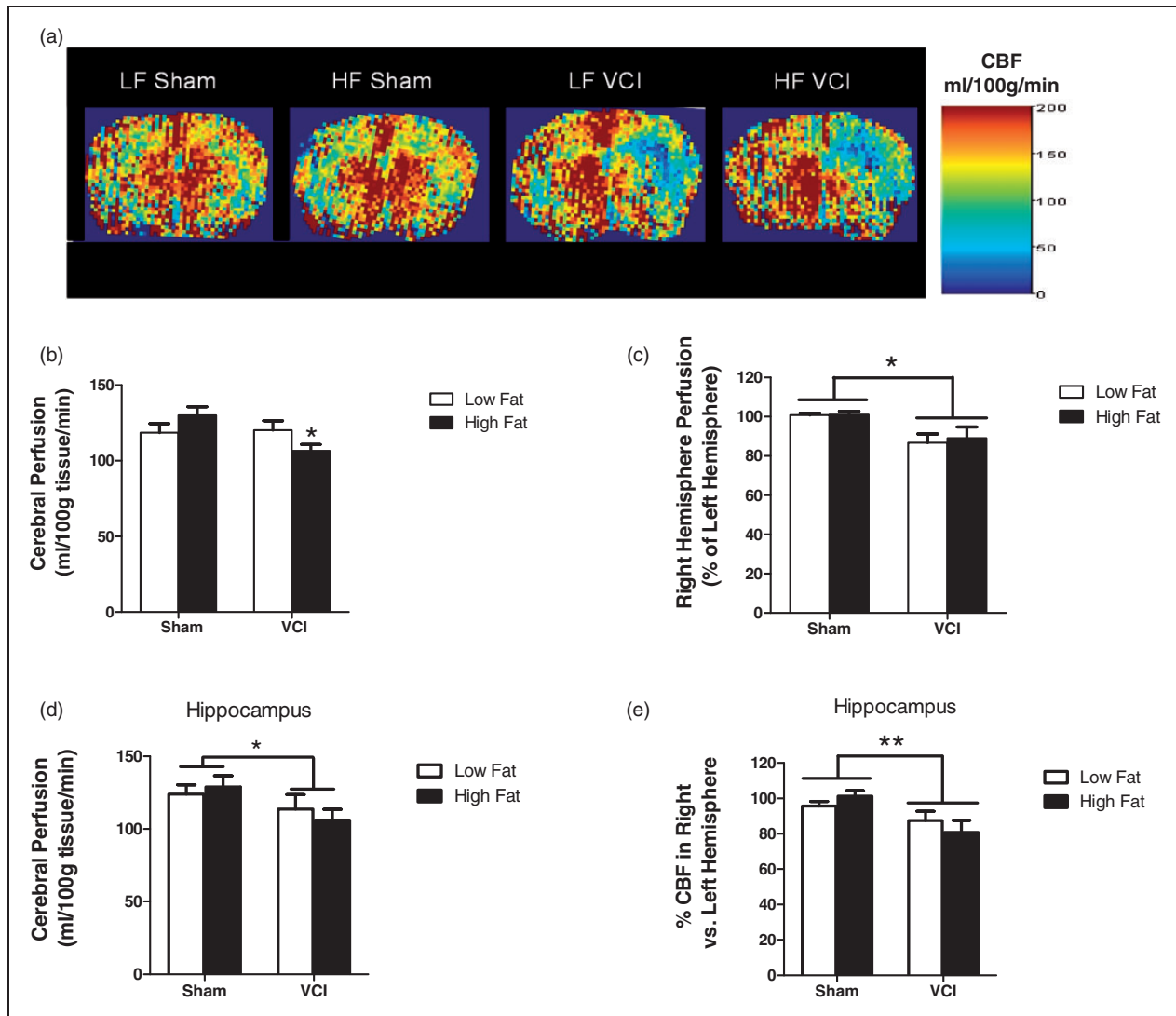


Figure 4. LF VCI mice show a unilateral decrease in cerebral blood flow (CBF), while HF VCI mice also display a global decrease in CBF that is exacerbated in the ischemic hemisphere. CBF was measured using ASL-MRI perfusion. (a) Representative CBF maps. (b) CBF in the right hemisphere was significantly reduced compared to CBF in the left hemisphere in LF VCI and HF mice (* $p < 0.01$ vs. LF Sham). (c) Whole brain CBF was significantly reduced in HF VCI mice compared to HF Sham mice (* $p < 0.05$ vs. HF Sham). (d) Whole hippocampus CBF was significantly reduced in VCI mice compared to Sham mice (* $p < 0.05$ vs. Sham). (e) CBF in the right hemisphere compared to the left was also significantly reduced in VCI mice compared to Sham mice (** $p < 0.01$ vs. Sham). $N = 6-7$ per group for all CBF measures.

HF diet alone had no effect on expression of Iba-1 or GFAP (Figure 6). VCI mice had increased Iba-1 and a trend towards increased GFAP ($p = 0.06$) in the CA1 region of the hippocampus in the right hemisphere compared to the left (Figure 6(a) and (c)). HF VCI mice showed the largest increase in Iba-1 expression in the CA1 in the right hemisphere (Figure 6(b) and (e)). Finally, we examined the density of neurons in the dentate, CA1, and CA3 regions of the hippocampus by counting the number of NeuN immunoreactive cells, a marker for mature neurons. No differences in neuronal density were observed between groups in the

CA1 or CA3 regions (data not shown). In the dentate, HF diet caused a decrease in the number of NeuN+ cells (Figure 7(a)). In HF VCI mice, this decrease was larger in the right hemisphere compared to the left (Figure 7(b) and (c)).

Discussion

The goal of the current study was to determine if diet-induced diabetes causes cognitive impairment by eliciting chronic cerebral hypoperfusion, or if it has flow-independent effects on neuronal function and

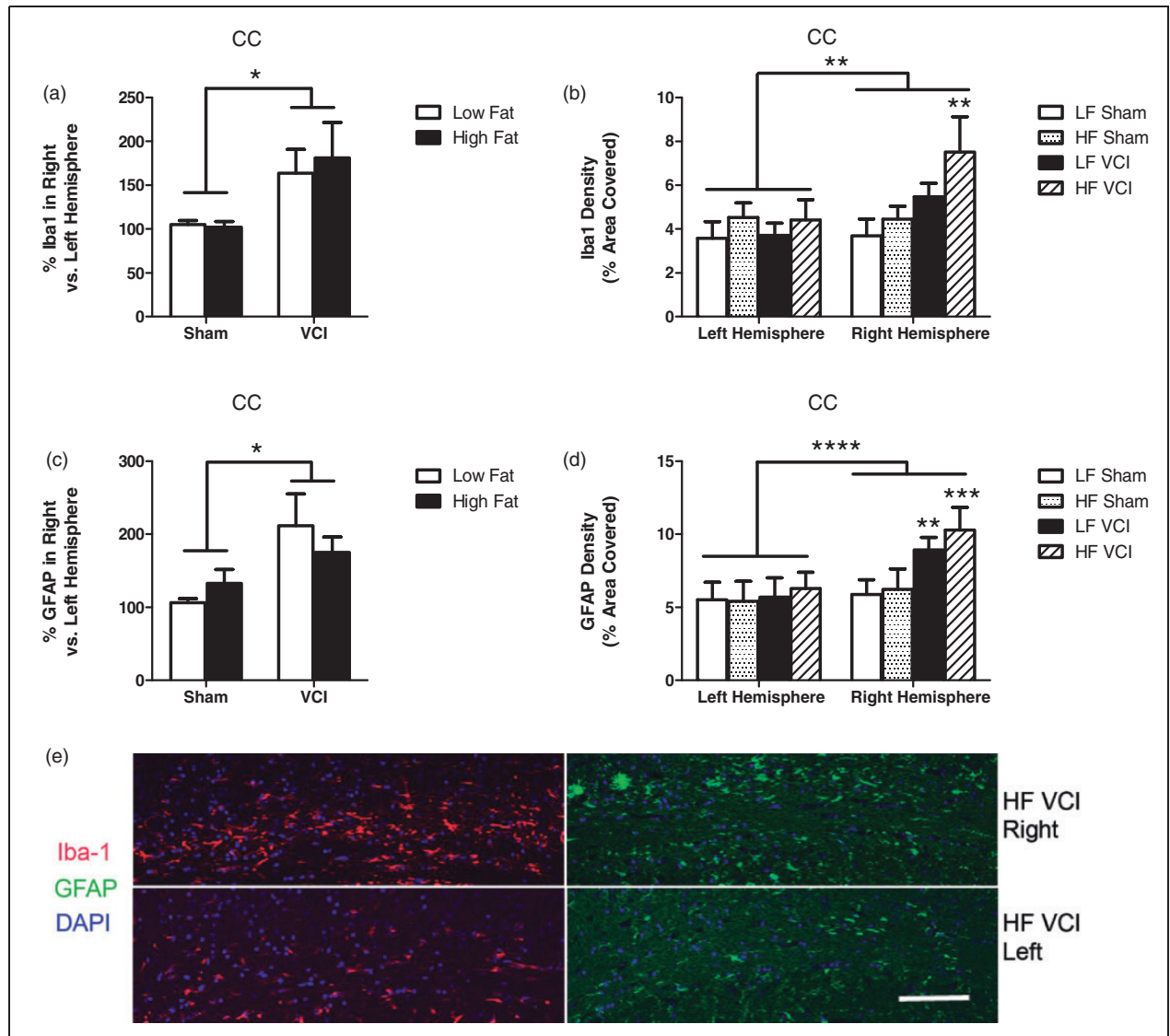


Figure 5. VCI mice have an increase in white matter reactive changes, which are exacerbated by HF diet. (a) VCI mice showed increased percent Iba-1 labeling in the right hemisphere corpus callosum (CC) compared to the left hemisphere CC, regardless of diet ($*p < 0.05$ vs. sham mice). (b) HF VCI mice showed increased Iba-1 labeling in the right hemisphere CC compared to LF VCI mice ($**p < 0.01$ vs. LF sham). (c) VCI mice showed increased percent GFAP labeling in the right hemisphere CC compared to the left hemisphere CC, regardless of diet ($*p < 0.05$ vs. sham mice). (d) HF VCI and LF VCI mice showed increased GFAP labeling in the right hemisphere CC compared to LF sham mice ($**p < 0.01$ vs. LF sham, $***p < 0.001$ vs. LF sham). $N = 6-7$ per group for all measures. (e) Representative images of Iba-1 and GFAP labeling in the CC of the right (ischemic; top images) and left (non-ischemic; bottom images) hemisphere of HF VCI mice. Scale bar = 100 μ m.

cognition. Our data suggest that chronic hypoperfusion due to UCCAO leads to cognitive impairment due to reductions in CBF and increased reactive changes in the both white matter and in the hippocampus. Similarly, diet-induced diabetes is also capable of causing cognitive impairments. However, the mechanism is not due to hypoperfusion, since CBF was not reduced by HF alone, although it does lead to neuronal loss in the hippocampus. In the presence of an HF diet, specific

cognitive impairments and hypoperfusion are exacerbated compared to UCCAO alone.

We characterized changes in CBF via ASL MRI, 3.5 months following VCI or sham surgery. UCCAO is known to cause large decreases in CBF in the ischemic hemisphere acutely,^{9,20} however, there has been conflicting evidence in the literature over whether UCCAO leads to permanent reductions in CBF, based on methodologies that assess cortical CBF in a

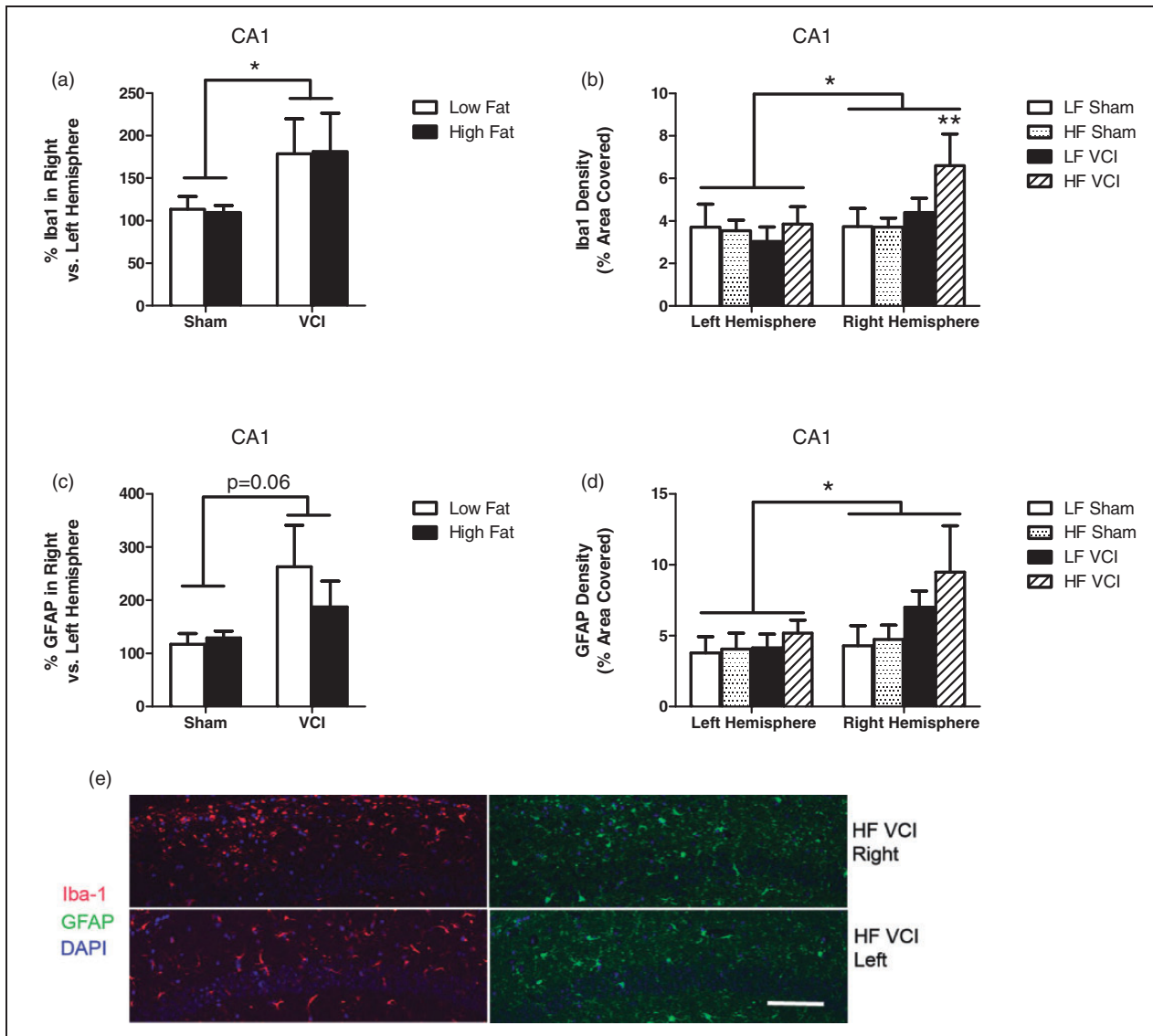


Figure 6. VCI mice have an increase in reactive changes in the CA1 region of the hippocampus, which are exacerbated by HF diet. Brains were collected 3.5 months after VCI or sham surgery and labeled for GFAP and Iba-1. (a) VCI mice showed increased the percent Iba-1 labeling in the right hemisphere CA1 region of the hippocampus compared to the left hemisphere CA1, regardless of diet (* $p < 0.05$ vs. sham mice). (b) HF VCI mice showed increased Iba-1 labeling in the right hemisphere CA1 compared to LF VCI mice (** $p < 0.01$ vs. LF sham). (c) VCI mice showed trend toward increased the percent GFAP labeling in the right hemisphere CA1 compared to the left hemisphere CA1, regardless of diet ($p = 0.06$ vs. sham mice). (d) VCI mice showed increased GFAP labeling in the right hemisphere CA1 compared to sham mice (* $p < 0.05$ vs. Sham). $N = 6-7$ per group for all measures. (e) Representative images of Iba-1 and GFAP labeling in the CA1 region of the right (ischemic; top images) and left (non-ischemic; bottom images) hemisphere of HF VCI mice. Scale bar = 100 μ m. Scale bar = 100 μ m.

small area of the brain.^{9,20} Recently, we reported that CBF, measured via MRI, is impaired in the ischemic hemisphere 4 months after UCAO surgery, but that total brain perfusion was unaltered. In the current study, LF VCI mice also showed a similar decrease in CBF in the right hemisphere with no change in total CBF. Others have shown that the lack of deficit in total brain perfusion may be due to capillary remodeling, pial arterial dilation, and collateralization.²⁰

However, in the current study we observed that mice on HF diet that received VCI surgery had both the expected decrease in CBF in the right hemisphere and a decrease in CBF in the whole brain. While blood pressure has been shown to be normal in mice on an HF diet (up to 16 months duration),²¹ cerebrovascular dysfunction has been reported in several mouse models of diabetes including the HF diet model.^{8,22} However, in the current study we did not find an effect of HF diet

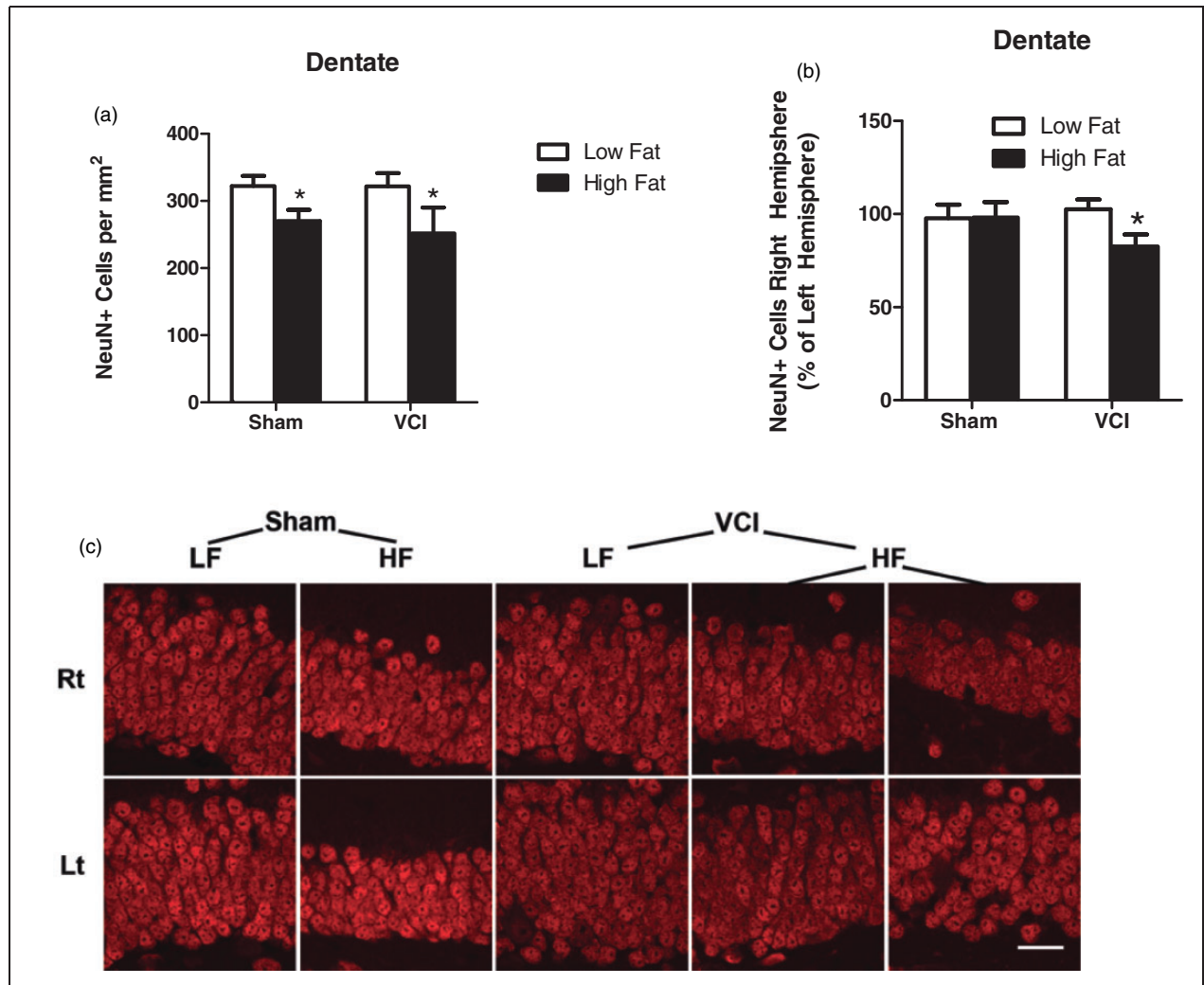


Figure 7. HF mice have decreased neuronal density in the dentate gyrus which is exacerbated by VCI surgery. Brains were collected 3.5 months after VCI or sham surgery and labeled for NeuN, a marker of mature neurons. (a) HF diet mice showed a decrease in the total number of NeuN+ cells in the dentate compared to LF diet mice (* $p < 0.05$ vs. LF mice). (b) HF VCI mice showed a decrease in the percentage of NeuN+ cells in the right hemisphere dentate gyrus compared to the left hemisphere (* $p < 0.05$ vs. LF Sham). $N = 6-7$ per group for all measures. (c) Representative images of NeuN labeling in the right (rt; ischemic; top images) and left (lt: non-ischemic; bottom images) hemisphere of mice from each group. Representative images for two mice from the HF VCI are shown in the far right columns. Scale bar = 20 μ m.

alone on CBF. It is possible that if the mice had been administered the HF diets longer than 6.5 months they may have eventually developed reductions in CBF. Although we did not detect changes in CBF in the HF diet mice, there is still a possibility that HF diet could elicit flow-independent microvascular changes such as changes in vascular reactivity, oxidative stress, capillary nutrient exchange, blood brain barrier function, or leukocyte/endothelial cell interactions. For example, HF diet in mice has been reported to impair endothelial mediated vasodilation in cerebral arteries,⁸ increase markers for superoxide and peroxynitrite production,^{8,23} alterations in blood brain barrier function,²³ and increase immune cell recruitment.²⁴

Many of these negative vascular changes, which have been shown to increase with age in the HF diet model,²³ would not have been detected in the current study but could have contributed to cognitive impairment observed. However, the lack of change in CBF in our diabetic mouse model is in agreement with previous work showing that diabetes does not alter blood flow in cerebral microvessels during normal conditions, but does cause alternations after a vascular insult.²⁵ Similarly, in our study with a combination of the HF diet and VCI surgery CBF was decreased. Therefore, it is possible that the diabetic mice were unable to fully compensate for the decrease in CBF in the right hemisphere following UCAO due to reported decreases in

cerebrovascular reactivity that occur in diabetes.^{8,22} Our current study shows that UCCAO causes impairments in nonspatial memory. Specifically, we detected deficits in the NORT. In agreement with our previous study,¹³ we did not observe a deficit in spatial memory performance in the MWM or in cued or contextual fear conditioning tests with VCI surgery alone. These findings are supported by several other studies that failed to find statistically significant differences in spatial memory in the MWM after UCCAO in mice.^{10,12} As previously observed,¹³ UCCAO surgery alone did not cause alternations in activity or anxiety-related behavior between groups.

We found that UCCAO causes an increase in reactive changes in both white and grey matter. Specifically, we found increased GFAP+ reactive astrocytes and Iba-1+ activated microglia in the right (ischemic) hemisphere of VCI mice in both the CC and the CA1 region of the hippocampus. These findings are in agreement with previous studies, which have shown that these markers are increased following UCCAO in mice.^{9,11} Further, these reactive markers have also been shown to be increased in other mouse models of VCI including the bilateral stenosis^{26,27} and asymmetric carotid stenosis.²⁸

Long-term HF diet also caused cognitive impairments. Specifically, we detected impairments in nonspatial memory in the NORT, spatial memory in the MWM, and associative learning in the cued fear conditioning task. Others have also reported cognitive deficits following long-term HF diet^{6,7} and in other rodent models of diabetes.²⁹ Cognitive deficits have also been reported in diabetic individuals.³ Type 2 diabetes is associated with a variety of pathologies that might contribute to the cognitive impairment including reduced endothelial function, greater incident of white matter damage, lower CBF, increased brain atrophy, increased infarcts, and neural slowing compared to healthy controls.^{1,2} Our results show that HF diet/diabetes also causes a reduction in neuronal density in the dentate gyrus of the hippocampus, a key area for adult neurogenesis. Reduced neurogenesis in this region could play a role in the cognitive dysfunction observed. In fact, reduced hippocampal neurogenesis has been reported in several rodent models of diabetes.^{30,31}

Our results show that HF diet causes cognitive deficits and exacerbates pathology following chronic cerebral hypoperfusion. HF VCI mice showed specific deficits in spatial and associative memory in the MWM and cued fear conditioning tasks, respectively, that LF VCI mice did not. Further, HF VCI mice showed a decrease in total brain CBF that was not present in LF VCI mice. This effect is likely due to the negative effects of diabetes on cerebrovascular function.^{8,22} In addition, reduced neuronal density in the dentate gyrus was observed in HF VCI mice but not

in LF VCI mice. Glial activation was also enhanced in the white and grey matter of HF VCI mice, and thus could have contributed to the cognitive deficits observed in these mice. Taken together, these data support the conclusion that diabetes induced by HF diet increases specific cognitive deficits and VCI-like pathology in mice following chronic hypoperfusion. Our results are supported by a very recent study in rats showing that diabetes increased specific cognitive deficits and neuronal loss following bilateral common carotid artery occlusion.³² Thus, diabetes appears to worsen specific cognitive deficits and underlying pathology following chronic hypoperfusion in multiple surgical models and species.

One limitation of the HF diet model of diabetes used in the current study is that experimenters could not be blinded to dietary status during surgery, behavior testing, and MRI due to the difference in food color, body weight, and general appearance of mice. Two measures were taken to minimize potential bias to address this limitation. First, all mice were assigned tail tattoo numbers prior to dietary intervention and these numbers were used for subsequent assignment to surgical treatment groups and MRI groups. Second, data analysis was conducted by experimenters blinded to both dietary status and surgical group.

In summary, we found that VCI and ~~HF~~ independently caused cognitive impairments, but the mechanisms are likely different. Specifically, both insults caused impaired memory. However, only UCCAO, but not HF diet, reduced CBF, and increased reactive changes in the white matter and hippocampus. Further, only HF diet, but not UCCAO, reduced neuronal density in the hippocampus. We conclude that insults caused by HF diet and chronic hypoperfusion are mechanistically different processes, although they share common features that target vulnerable brain regions, such as the hippocampus. Our results suggest that improving cerebral perfusion may prevent cognitive impairments, but that preventative measures will be much more successful if dietary modifications and/or diabetes management are addressed as well.

Funding

This work was supported by R21AG043857 (N.J.A.), R01NS070837 (N.J.A.), F32NS082017 (K.L.Z.) National Science Foundation, SMA-1408653 (LAJ), T32-HL094294 (L.A.J.), Oregon Tax Check-off Grant Alzheimer's Research Fund (L.A.J.), the Collins Medical Trust (L.A.J.), and the development account of J.R.

Declaration of conflicting interests

The author(s) declared no potential conflicts of interest with respect to the research, authorship, and/or publication of this article.

Authors' contributions

K.L.Z., L.A.J., M.R.G., M.M.P., J.R., and N.J.A. designed the experiments and interpreted the data. K.L.Z., L.A.J., N.E.R., T.M., W.Z., X.N., and M.M.P. collected the data. K.L.Z., L.A.J., N.E.R., T.M., F.N.A., and C.H. analyzed the data. K.L.Z., L.A.J., M.R.G., M.M.P., J.R. and N.J.A. prepared the manuscript. N.J.A. is the guarantor of the work and, as such, had full access to all the data in the study and takes full responsibility for the integrity of the data and accuracy of the data analysis.

References

1. McCrimmon RJ, Ryan CM and Frier BM. Diabetes and cognitive dysfunction. *Lancet* 2012; 379: 2291–2299.
2. Biessels GJ, Staekenborg S, Brunner E, et al. Risk of dementia in diabetes mellitus: a systematic review. *Lancet Neurol* 2006; 5: 64–74.
3. van Harten B, Oosterman J, Muslimovic D, et al. Cognitive impairment and MRI correlates in the elderly patients with type 2 diabetes mellitus. *Age Ageing* 2007; 36: 164–170.
4. Roberts RO, Knopman DS, Przybelski SA, et al. Association of type 2 diabetes with brain atrophy and cognitive impairment. *Neurology* 2014; 82: 1132–1141.
5. Winzell MS and Ahren B. The high-fat diet fed mouse: a model for studying mechanisms and treatment of impaired glucose tolerance and type 2 diabetes. *Diabetes* 2004; 53: S215–S219.
6. Morrison CD, Pistell PJ, Ingram DK, et al. High fat diet increases hippocampal oxidative stress and cognitive impairment in aged mice: implications for decreased Nrf2 signaling. *J Neurochem* 2010; 114: 1581–1589.
7. Jeon BT, Jeong EA, Shin HJ, et al. Resveratrol attenuates obesity-associated peripheral and central inflammation and improves memory deficit in mice fed a high-fat diet. *Diabetes* 2012; 61: 1444–1454.
8. Lynch CM, Kinzenbaw DA, Chen X, et al. Nox2-derived superoxide contributes to cerebral vascular dysfunction in diet-induced obesity. *Stroke* 2013; 44: 3195–3201.
9. Yoshizaki K, Adachi K, Kataoka S, et al. Chronic cerebral hypoperfusion induced by right unilateral common carotid artery occlusion causes delayed white matter lesions and cognitive impairment in adult mice. *Exp Neurol* 2008; 210: 585–591.
10. Zhao Y, Gu JH, Dai CL, et al. Chronic cerebral hypoperfusion causes decrease of O-GlcNAcylation, hyperphosphorylation of tau and behavioral deficits in mice. *Front Aging Neurosci* 2014; 6: 10.
11. Ma J, Xiong JY, Hou WW, et al. Protective effect of carnosine on subcortical ischemic vascular dementia in mice. *CNS Neurosci Ther* 2012; 18: 745–753.
12. Lee JS, Im DS, An YS, et al. Chronic cerebral hypoperfusion in a mouse model of Alzheimer's disease: an additional contributing factor of cognitive impairment. *Neurosci Lett* 2011; 489: 84–88.
13. Zuloaga KL, Zhang W, Yeiser LA, et al. Neurobehavioral and imaging correlates of hippocampal atrophy in a mouse model of vascular cognitive impairment. *Transl Stroke Res* 2015; ■■■■■■.
14. Benice TS and Raber J. Object recognition analysis in mice using nose-point digital video tracking. *J Neurosci Methods* 2008; 168: 422–430.
15. Maren S. Neurobiology of Pavlovian fear conditioning. *Annu Rev Neurosci* 2001; 24: 897–931.
16. Kim SG. Quantification of relative cerebral blood flow change by flow-sensitive alternating inversion recovery (FAIR) technique: application to functional mapping. *Magn Reson Med* 1995; 34: 293–301.
17. Lein ES, Hawrylycz MJ, Ao N, et al. Genome-wide atlas of gene expression in the adult mouse brain. *Nature* 2007; 445: 168–176.
18. Iadecola C. The pathobiology of vascular dementia. *Neuron* 2013; 80: 844–866.
19. Jack CR, Petersen RC, Xu YC, et al. Medial temporal atrophy on MRI in normal aging and very mild Alzheimer's disease. *Neurology* 1997; 49: 786–794.
20. Guo H, Itoh Y, Toriumi H, Yamada S, et al. Capillary remodeling and collateral growth without angiogenesis after unilateral common carotid artery occlusion in mice. *Microcirculation* 2011; 18: 221–227.
21. Calligaris SD, Lecanda M, Solis F, et al. Mice long-term high-fat diet feeding recapitulates human cardiovascular alterations: an animal model to study the early phases of diabetic cardiomyopathy. *PLoS One* 2013; 8: e60931.
22. Kitayama J, Faraci FM, Gunnnett CA, et al. Impairment of dilator responses of cerebral arterioles during diabetes mellitus: role of inducible NO synthase. *Stroke* 2006; 37: 2129–2133.
23. Tucek Z, Toth P, Sosnowska D, et al. Obesity in aging exacerbates blood–brain barrier disruption, neuroinflammation, and oxidative stress in the mouse hippocampus: effects on expression of genes involved in beta-amyloid generation and Alzheimer's disease. *J Gerontol A Biol Sci Med Sci* 2014; 69: 1212–1226.
24. Buckman LB, Hasty AH, Flaherty DK, et al. Obesity induced by a high-fat diet is associated with increased immune cell entry into the central nervous system. *Brain Behav Immun* 2014; 35: 33–42.
25. Tennant KA and Brown CE. Diabetes augments in vivo microvascular blood flow dynamics after stroke. *J Neurosci* 2013; 33: 19194–19204.
26. Dong YF, Kataoka K, Toyama K, et al. Attenuation of brain damage and cognitive impairment by direct renin inhibition in mice with chronic cerebral hypoperfusion. *Hypertension* 2011; 58: 635–642.
27. Toyama K, Koibuchi N, Uekawa K, et al. Apoptosis signal-regulating kinase 1 is a novel target molecule for cognitive impairment induced by chronic cerebral hypoperfusion. *Arterioscler Thromb Vasc Biol* 2014; 34: 616–625.
28. Hattori Y, Enmi J, Kitamura A, et al. A novel mouse model of subcortical infarcts with dementia. *J Neurosci* 2015; 35: 3915–3928.
29. Li XL, Aou S, Oomura Y, Hori N, et al. Impairment of long-term potentiation and spatial memory in leptin receptor-deficient rodents. *Neuroscience* 2002; 113: 607–615.

30. [Lang BT, Yan Y, Dempsey RJ, et al. Impaired neurogenesis in adult type-2 diabetic rats. *Brain Res* 2009; 1258: 25–33.](#)
31. [Beauquis J, Saravia F, Coulaud J, et al. Prominently decreased hippocampal neurogenesis in a spontaneous model of type 1 diabetes, the nonobese diabetic mouse. *Exp Neurol* 2008; 210: 359–367.](#)
32. Kwon KJ, Lee EJ, Kim MK, et al. Diabetes augments cognitive dysfunction in chronic cerebral hypoperfusion by increasing neuronal cell death: implication of cilostazol for diabetes mellitus-induced dementia. *Neurobiol Dis* 2015; 73: 12–23.